Nanomaterials

Lecture 19: Nanoelectromechanical Systems

Detecting Biomolecules with Nanomechanics

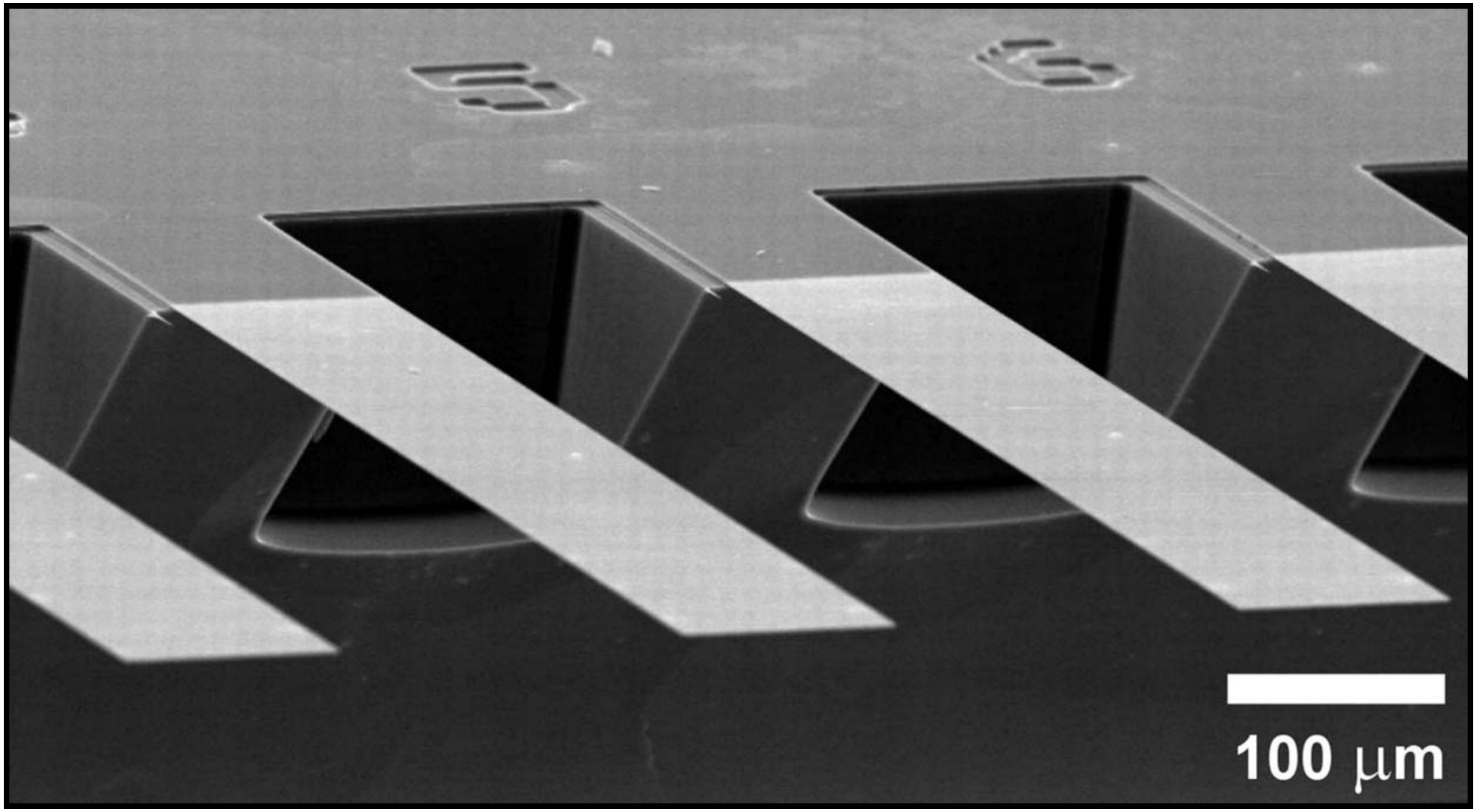

J. Fritz, *et al.*, *Science*, **288**, 316 (2000).

Detecting Biomolecules with Nanomechanics

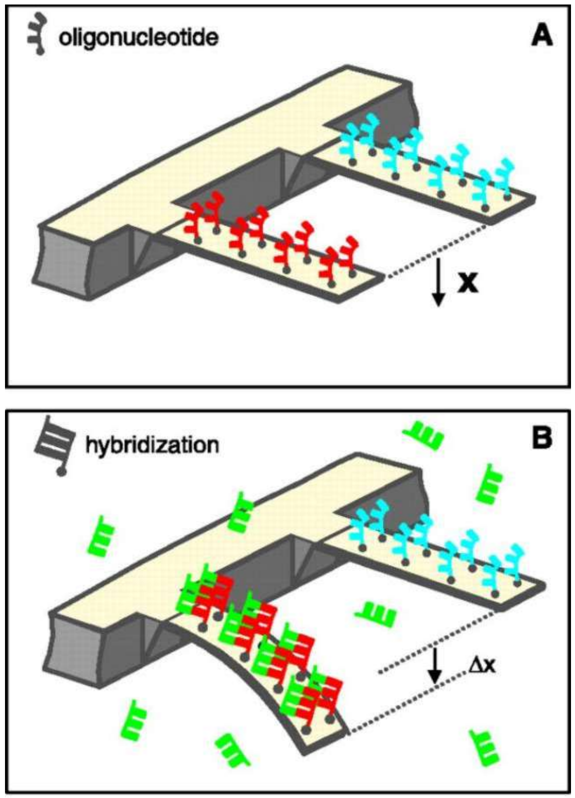

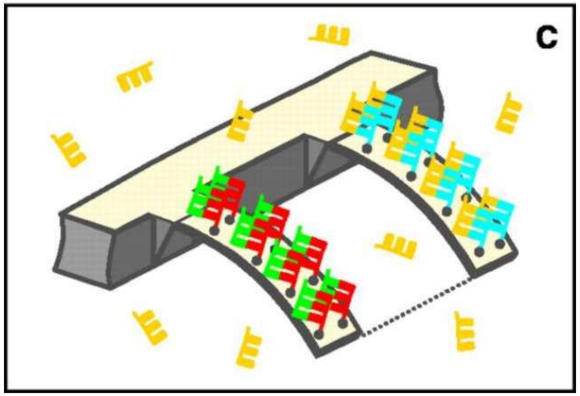

Changes in surface stress upon hybridization lead to cantilever deflection

J. Fritz, *et al.*, *Science*, **288**, 316 (2000).

Powering a Nanodevice with a Biomolecular Motor

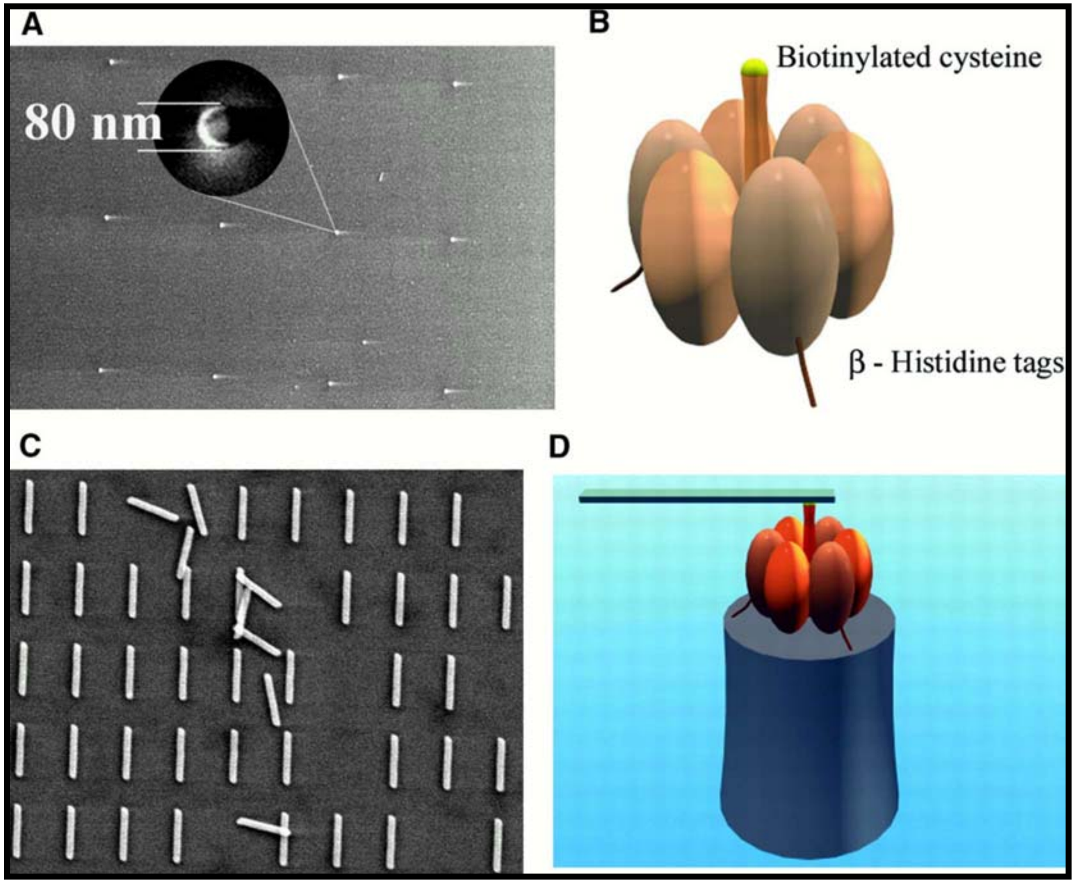

- Bind F_1-ATPase to nickel pillars
- Bind nickel nanopropellers to rotating component of F_1-ATPase
- Initiate rotation with ATP and inhibit rotation with sodium azide

R. K. Soong, *et al.*, *Science*, **290**, 1555 (2000).

Powering a Nanodevice with a Biomolecular Motor

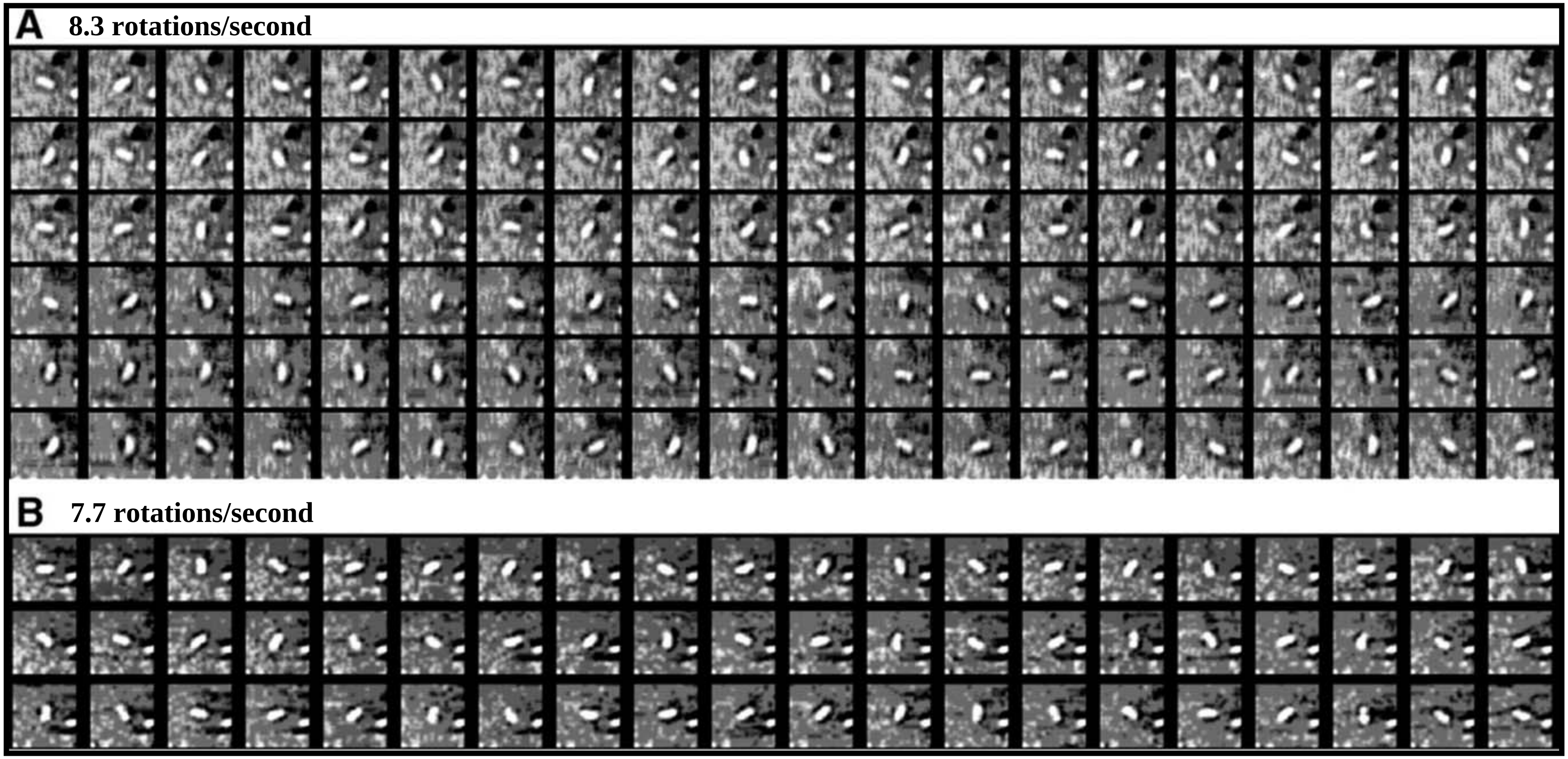

R. K. Soong, *et al.*, *Science*, **290**, 1555 (2000).

Single Molecule Rotors

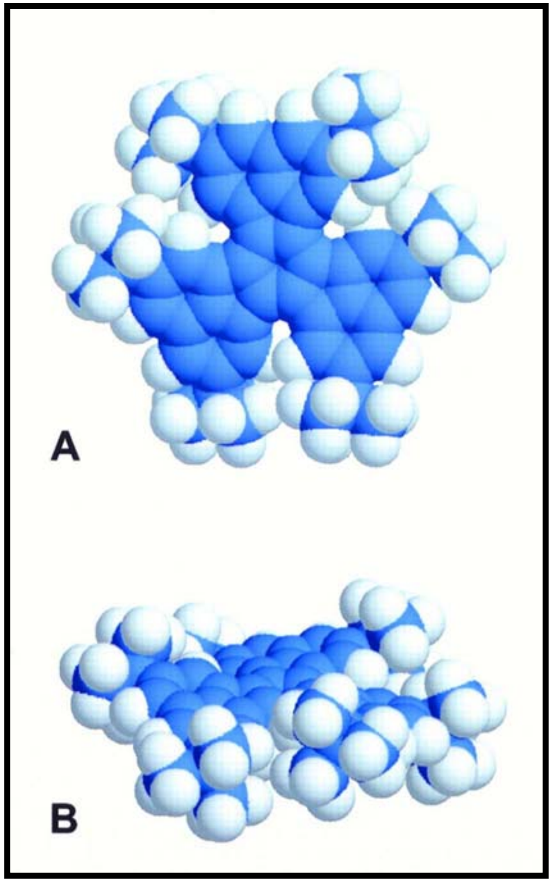

Hexa-*tert*-butyl decacyclene (HB-DC)

J. K. Gimzewski, *et al.*, *Science*, **281**, 531 (1998).

Monolayer of HB-DC on Cu(100)

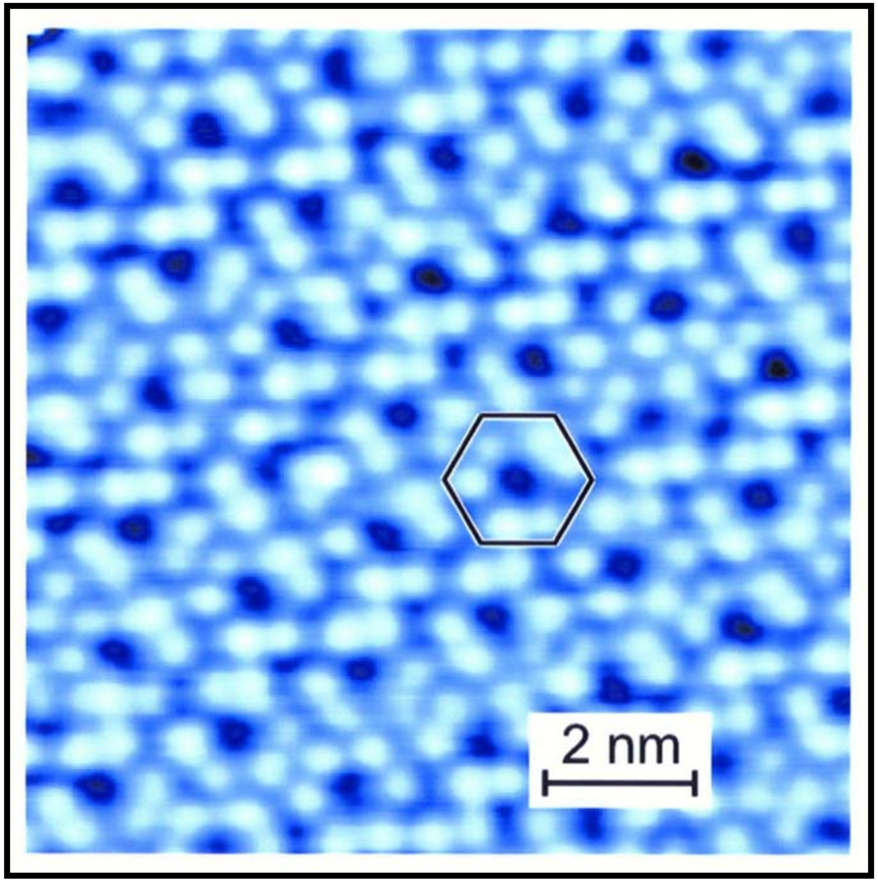

J. K. Gimzewski, *et al.*, *Science*, **281**, 531 (1998).

Rotational and Immobilized States of HB-DC

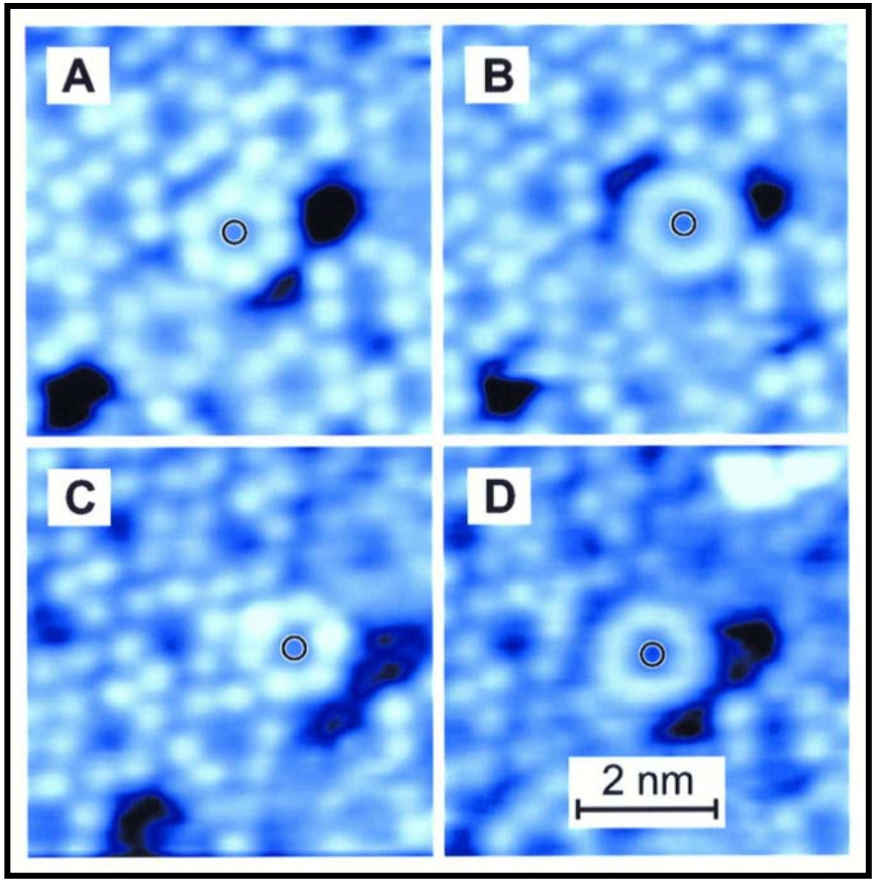

J. K. Gimzewski, *et al.*, *Science*, **281**, 531 (1998).

Rotational and Immobilized States of HB-DC

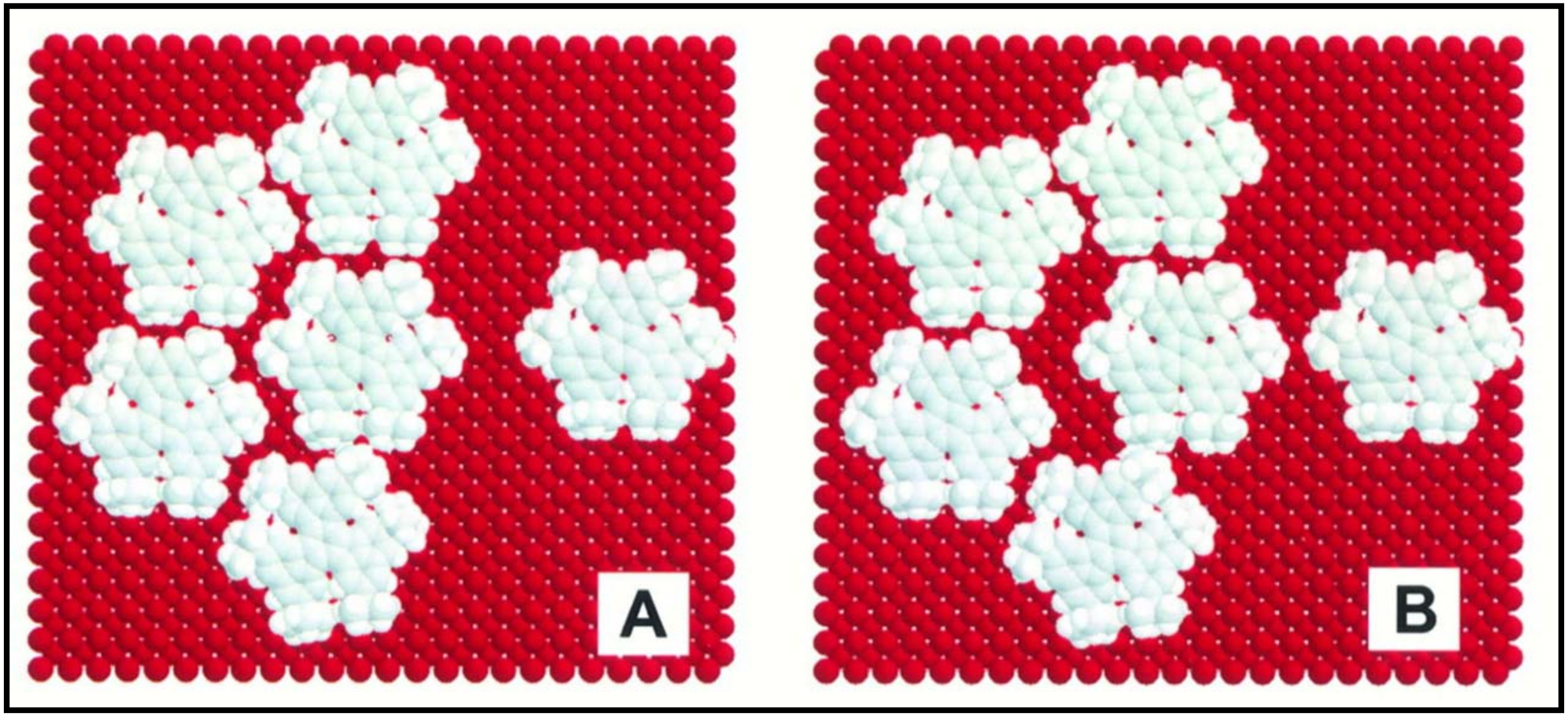

→ Rotational and immobilized states are separated by only 0.26 nm

J. K. Gimzewski, *et al.*, *Science*, **281**, 531 (1998).

Rotational and Immobilized States of HB-DC

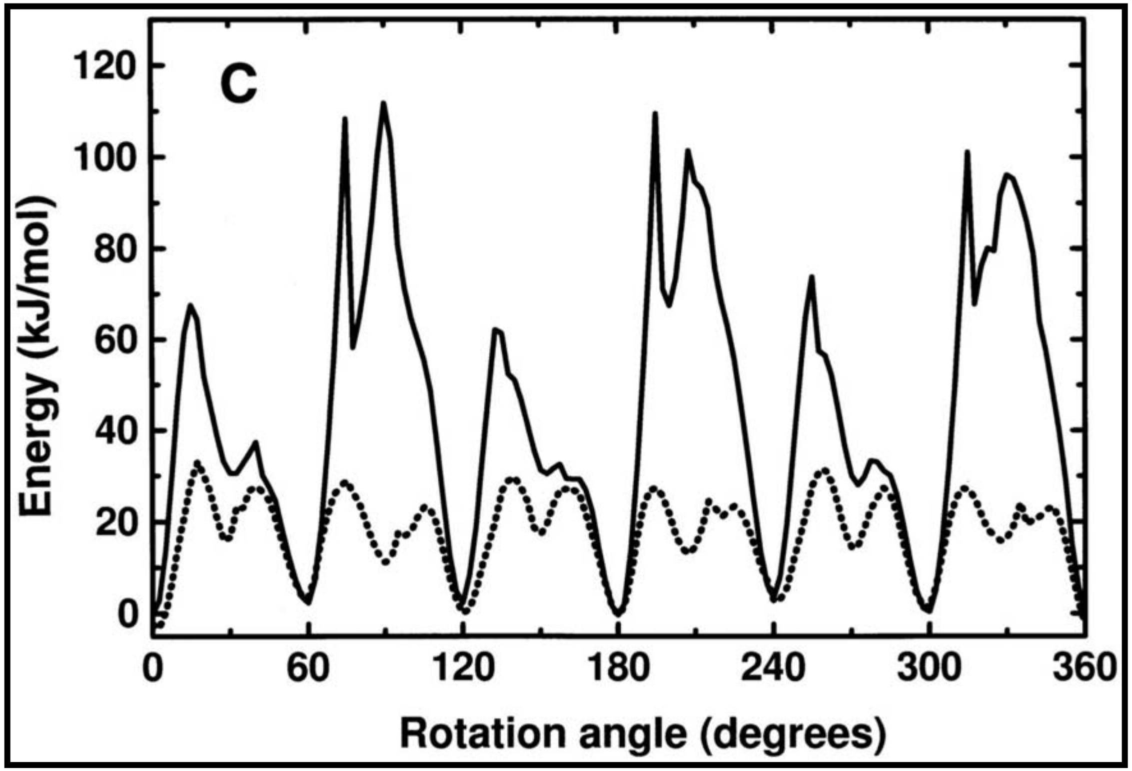

Dotted line = rotational state; Solid line = immobilized state

J. K. Gimzewski, *et al.*, *Science*, **281**, 531 (1998).

Simulations of Molecular Rotors

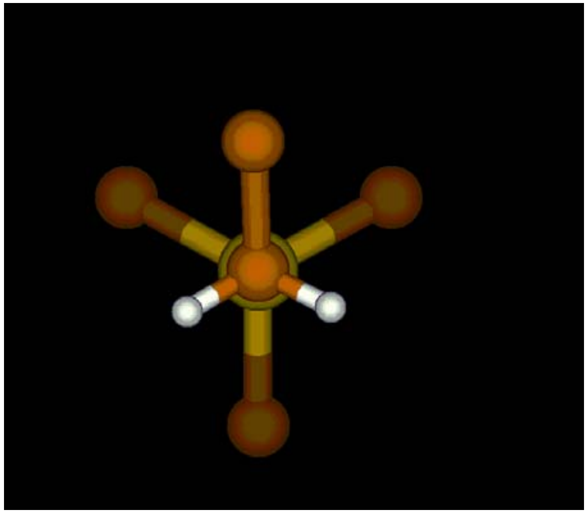
Small Kinetic Energy

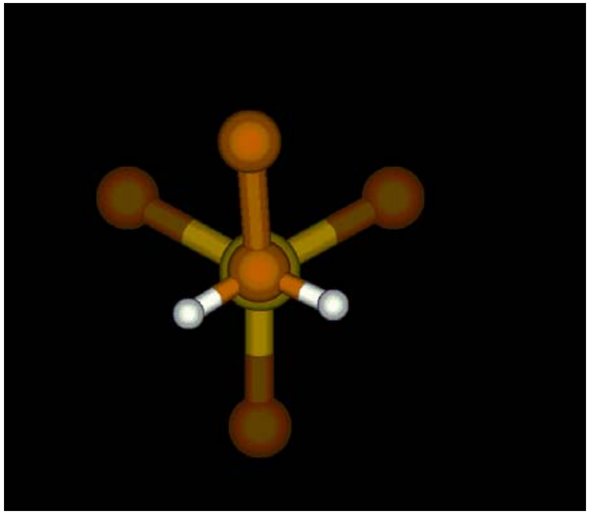
Intermediate Kinetic Energy

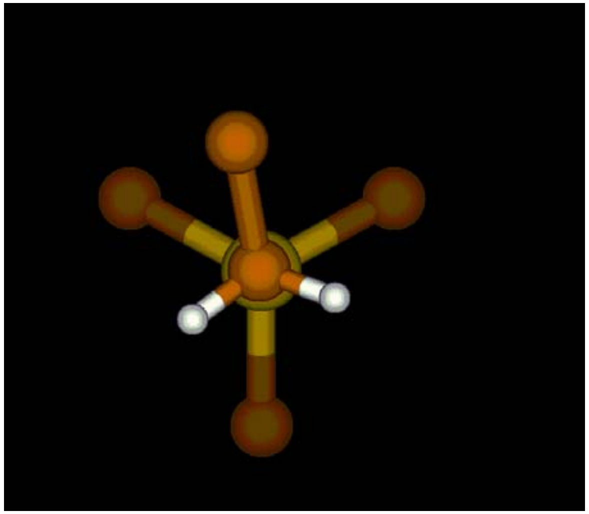
Large Kinetic Energy

Single Molecule Rotors on Si(100)

Stationary

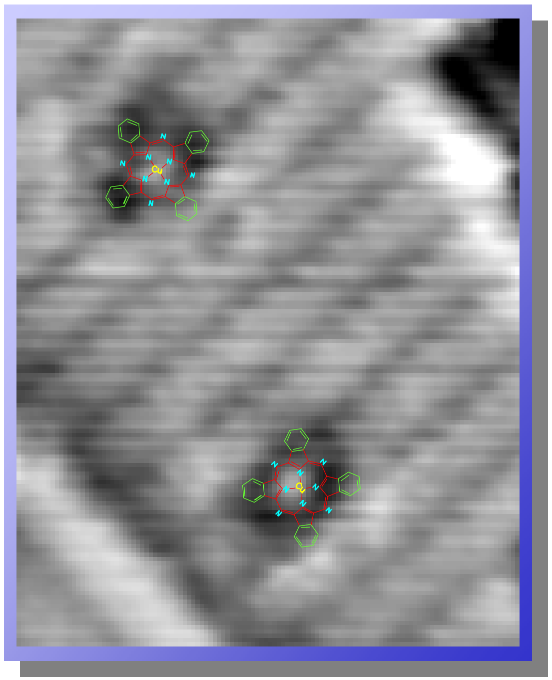

CuPc bonded by central Cu atom.

Rotating

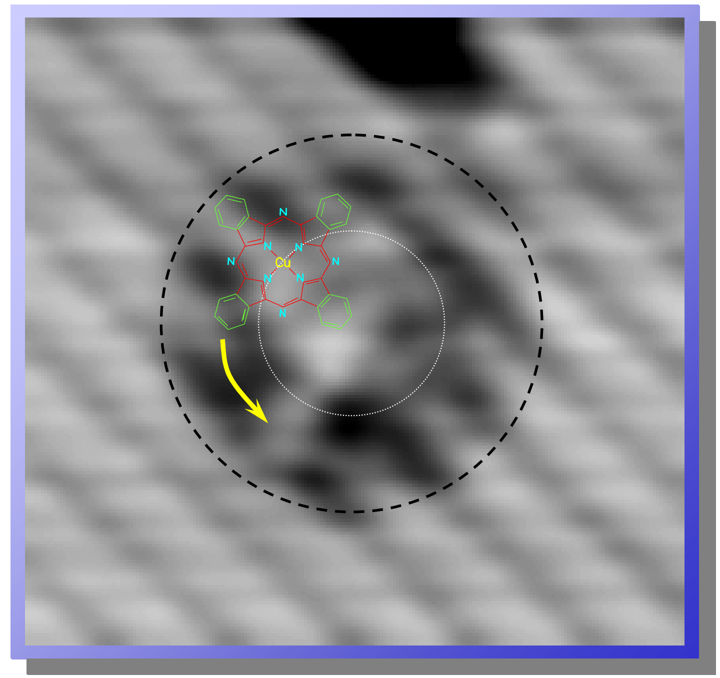

NH_3-reacted CuPc forms weak bond via outer phenyl group.

M. C. Hersam, *et al.*, *Nanotechnology*, **11**, 70 (2000).

Single Molecule Rotors on Si(100)

CuPc

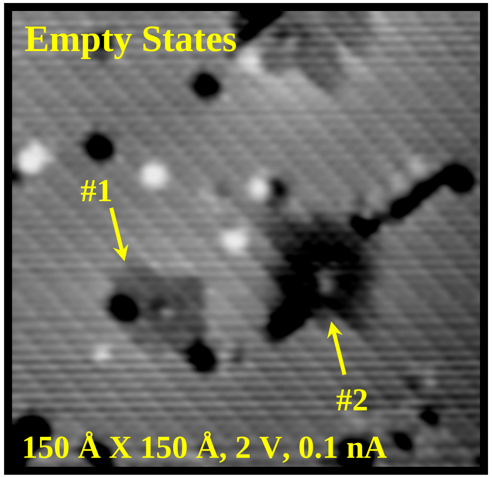

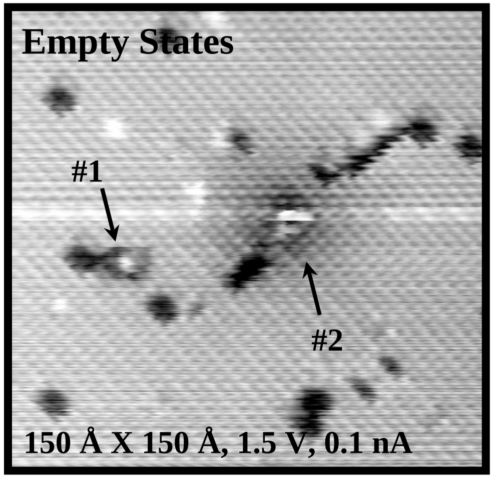

CuPc can either be fixed or rotating on the surface.

CuPc + NH_3

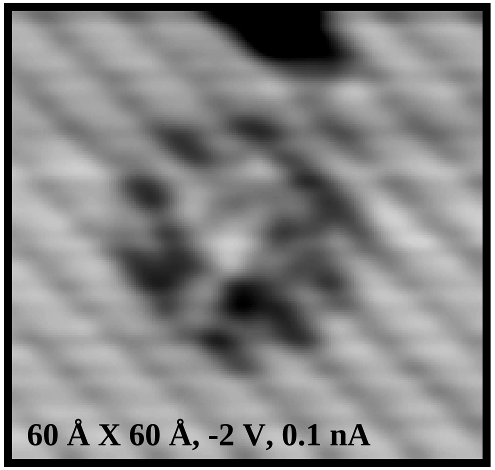

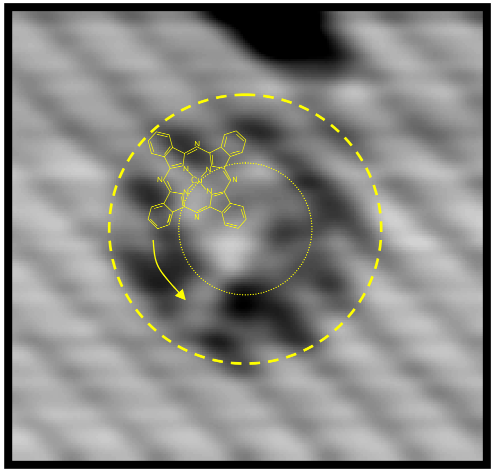

NH_3-CuPc always rotates on the surface.

Jann-Teller effect may be playing a role.

STM Barrier Height Imaging of Altitudinal Rotors on Au(111)

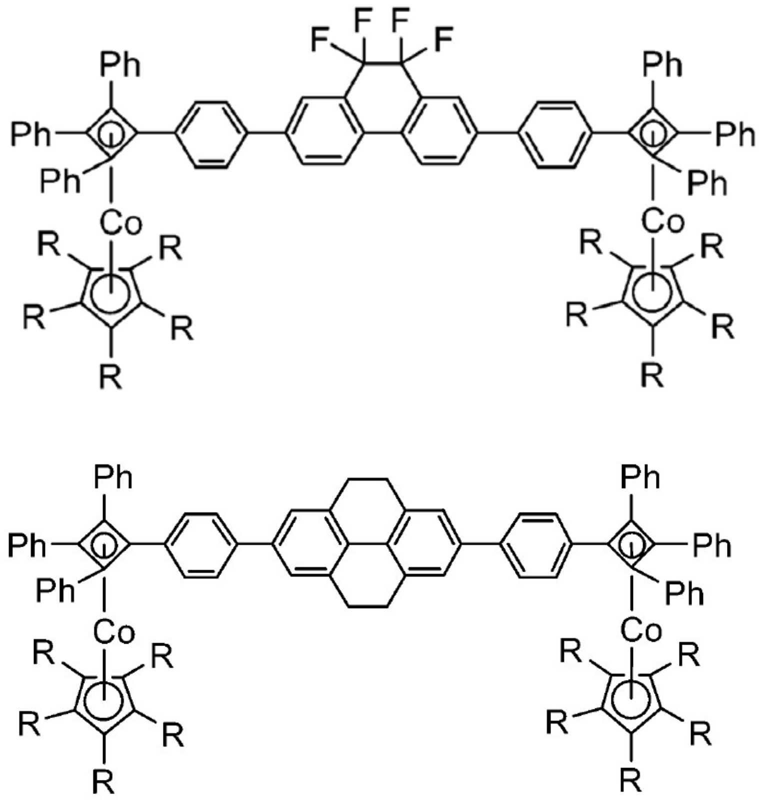

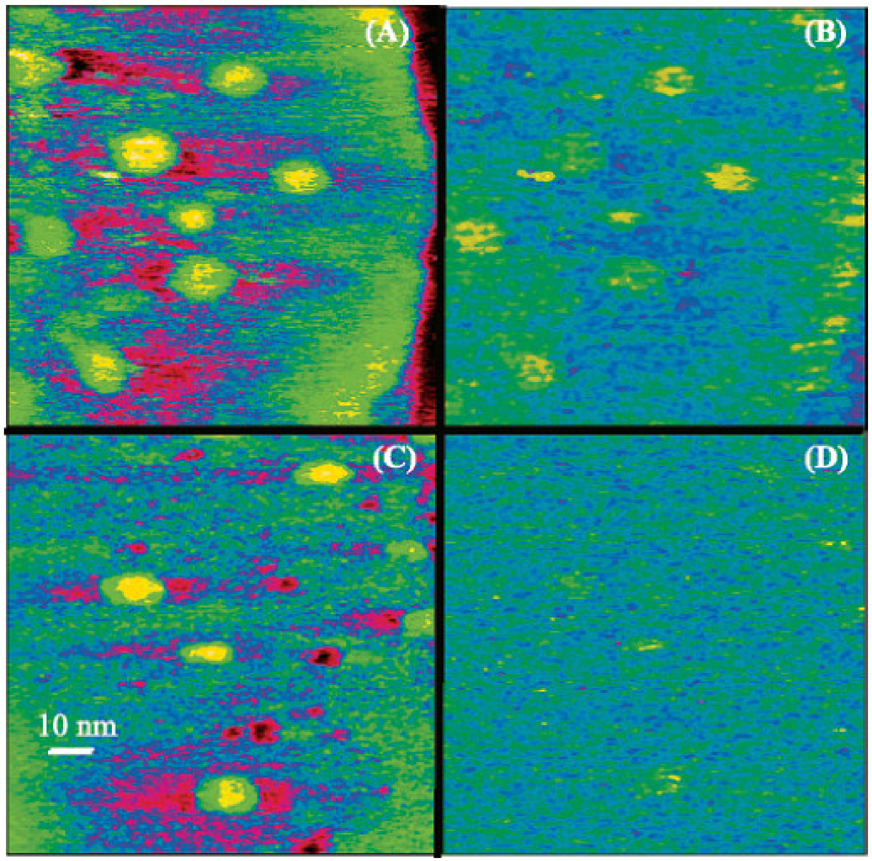

JACS, **126**, 4540 (2004).

Schematic of a Three-Terminal Electromechanical Device

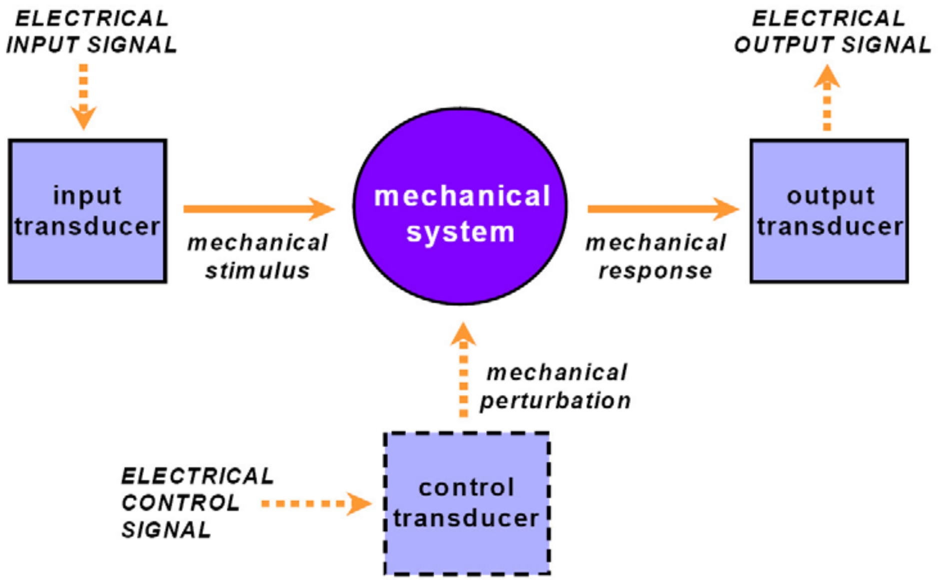

Figure 1. Schematic representation of a three-terminal electromechanical device.

How do we optimize performance? Does nano really help?

M. L. Roukes, *Tech. Digest. Solid State Sensor and Actuator Workshop* (2000)

Fundamental Frequencies for Mechanical Resonators

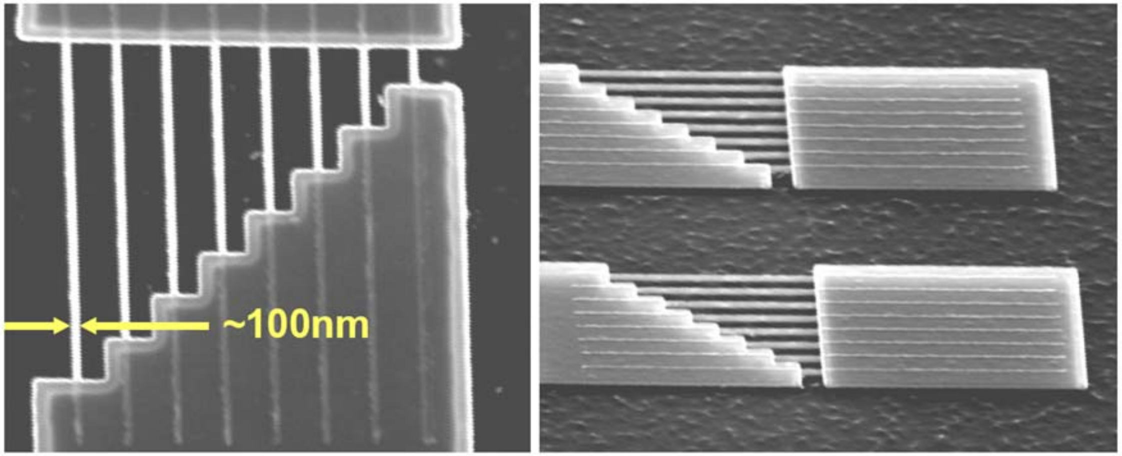

Fundamental frequency scales with Young's modulus

Table 1: Fundamental Frequency *vs.* Geometry for *SiC*, [Si], and (GaAs) Mechanical Resonators

Boundary Conditions	Resonator Dimensions ($L \times w \times t$, *in* μm)			
	100 × 3 × 0.1	*10 × 0.2 × 0.1*	*1 × 0.05 × 0.05*	*0.1 × 0.01 × 0.01*
Both Ends Clamped or Free	*120 KHz* [77] (42)	*12 MHz* [7.7] (4.2)	*590 MHz* [380] (205)	*12 GHz* [7.7] (4.2)
Both Ends Pinned	*53 KHz* [34] (18)	*5.3 MHz* [3.4] (1.8)	*260 MHz* [170] (92)	*5.3 GHz* [3.4] (1.8)
Cantilever	*19 KHz* [12] (6.5)	*1.9 MHz* [1.2] (0.65)	*93 MHz* [60] (32)	*1.9 GHz* [1.2] (0.65)

M. L. Roukes, *Tech. Digest. Solid State Sensor and Actuator Workshop* (2000)

Comments on Fundamental Frequencies for Mechanical Resonators

Molecular dynamics simulations show that the continuum mechanics description holds down to a length scale of ~10 lattice constants.

However, the calculations in the previous table assume zero internal strain, which is certainly not the case in many multi-layered devices.

Furthermore, surface non-idealities may lead to further deviations from ideal continuum calculations.

M. L. Roukes, *Tech. Digest. Solid State Sensor and Actuator Workshop* (2000)

Scaling of the Quality Factor

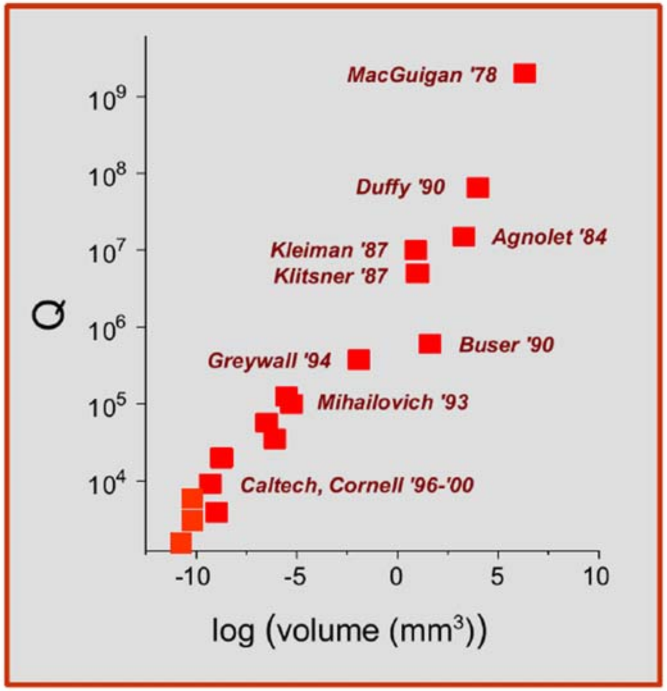

Figure 2. Q's in mechanical resonators varying in size from the macroscale to the nanoscale. *The data follow a trend showing a decrease in Q that occurs, roughly, with linear dimension — i.e. with the increasing surface-to-volume ratio of small structures, (After D. Harrington, unpublished.)*

Q Factors on the order of $10^3 – 10^5$ are achievable in NEMS structures.

Lower Q implies higher bandwidth.

M. L. Roukes, *Tech. Digest. Solid State Sensor and Actuator Workshop* (2000)

Estimating Power Levels for NEMS

Multiply thermal energy by bandwidth of the resonator to estimate the signal power that is needed to overcome thermal fluctuations.

↓

$$P_{min} \sim k_B T \omega_0 / Q$$

(Estimates energy exchange between the resonant mode and the thermal environment)

M. L. Roukes, *Tech. Digest. Solid State Sensor and Actuator Workshop* (2000)

Typical Power Levels for NEMS

Table 2: Representative operating power levels for NEMS.

f_0	Q	P_{min}	$10^6 \cdot P_{min}$
100 MHz	10,000	40 aW	40 pW
"	100,000	4 aW	4 pW
1 GHz	10,000	0.4 f W	0.4 nW
"	100,000	40 aW	40 pW

Low power operation is achievable even for devices that exceed minimum levels by a factor of 10^6.

M. L. Roukes, *Tech. Digest. Solid State Sensor and Actuator Workshop* (2000)

Responsivity and Aspect Ratios

High frequencies are achievable at the micron scale for low aspect ratio structures.

However, low aspect ratio structures possess large force constants, which leads to many disadvantages:

(1) Higher power level of operation
(2) Difficulty in controlling via applied mechanical forces
(3) Q factor is reduced due to acoustic coupling to boundaries

M. L. Roukes, *Tech. Digest. Solid State Sensor and Actuator Workshop* (2000)

Mass Sensitivity

Mass sensitivity ~ *m*/*Q*

where m is the active mass of the resonator

Table 3: Important attributes for a family of doubly-clamped Si beams. *The effective force constant, k_{eff}, is defined for point loading at the beam's center. S_X and S_F are the spectral densities for displacement and force noise from thermomechanical fluctuations; a noisy readout will degrade these ideal values. Nonlinear onset has been characterized using the criterion described in the text. The linear dynamic range (DR) is defined as the ratio of this onset to $\sqrt{(S_X\omega_0/Q)}$. Noise-matched cryogenic operation at 4K adds ~19dB to the linear DR values shown. Active mass is ~half the beam's mass for the fundamental mode. Mass sensitivity, measured in Daltons* (1D=1.7x10^{-24} g) *is for a half linewidth shift.*

Dimensions $L \times w \times t$, *(all in μm)*	**Resonator Attributes assuming *Q = 10,000* (100,000)**							
	Frequency $\omega_0/2\pi$	κ_{eff} ***(N/m)***	$S_x^{1/2}(\omega_0)$ ***at 300K*** ***(m/√Hz)***	***Nonlinear Onset,*** $\langle x_N \rangle$,***(m)***	***Linear DR (dB)***	$S_F^{1/2}(\omega_0)$ ***at 300K*** ***(N/√Hz)***	***Active Mass***	***Approx. Mass Sens., (D)***
$100 \times 3 \times 0.1$	*77 KHz*	*.007*	*2x10^{-10}* (7x10^{-10})	*5x10^{-7}*	*51* (51)	*3x10^{-16}* (5x10^{-17})	*40 pg*	*10^9* (10^8)
$10 \times 0.2 \times 0.1$	*7.7 MHz*	*0.5*	*3x10^{-12}* (8x10^{-12})	*5x10^{-7}*	*68* (68)	*1x10^{-16}* (4x10^{-17})	*0.3 pg*	*10^7* (10^6)
$1 \times 0.05 \times 0.05$	*380 MHz*	*16*	*7x10^{-14}* (2x10^{-13})	*3x10^{-8}*	*59* (59)	*1x10^{-16}* (3x10^{-17})	*3 fg*	*10^5* (10^4)
$0.1 \times 0.01 \times 0.01$	*7.7 GHz*	*25*	*4x10^{-14}* (1x10^{-13})	*5x10^{-9}*	*35* (35)	*3x10^{-17}* (9x10^{-18})	*10 ag*	*10^3* (10^2)

M. L. Roukes, *Tech. Digest. Solid State Sensor and Actuator Workshop* (2000)

Principal Engineering Challenges for NEMS

Pursuit of ultrahigh Q factors

Factors limiting Q include:

(a) Extrinsic mechanisms (e.g., air damping, clamping losses at supports, and coupling losses at transducers)
(b) Intrinsic mechanisms (e.g., bulk material defects, fabrication-induced surface damage, and surface adsorbates)

M. L. Roukes, *Tech. Digest. Solid State Sensor and Actuator Workshop* (2000)

Principal Engineering Challenges for NEMS

Surfaces

To date, Q factors have routinely scaled with resonator size independent of the material type.

This behavior suggests that the surfaces rather than the bulk are dominant.

Surface passivation is thus of critical importance.

M. L. Roukes, *Tech. Digest. Solid State Sensor and Actuator Workshop* (2000)

Principal Engineering Challenges for NEMS

Transducers

In MEMS, electrostatic actuators are commonplace. However, in NEMS, the capacitance decreases to levels comparable to spurious sources of background capacitance, thus limiting electrostatic actuation strategies.

Optical detection is also unachievable in NEMS as device sizes fall below the diffraction limit.

M. L. Roukes, *Tech. Digest. Solid State Sensor and Actuator Workshop* (2000)

Principal Engineering Challenges for NEMS

Reproducible nanofabrication

NEMS devices are extremely sensitive to mass changes.

Consequently, exceptional high tolerances are placed on nanofabrication in order to achieve predictable and reproducible device operation.

M. L. Roukes, *Tech. Digest. Solid State Sensor and Actuator Workshop* (2000)

Potential NEMS Engineering Solutions

Surfaces

Rather than attempting to passivate surface dangling bonds, attempt to use materials that are perfectly terminated (i.e., possess no dangling bonds)

This reasoning motivates the use of carbon nanotubes in NEMS.

M. L. Roukes, *Tech. Digest. Solid State Sensor and Actuator Workshop* (2000)

Potential NEMS Engineering Solutions

Novel displacement transducers

- Magnetomotive: Moving nanomagnet induces current flow in a nearby wire loop
- Direct magnetic detection of moving nanomagnet by superconducting quantum interference devices (SQUIDs)
- Piezoelectric detection/actuation
- Electron tunneling (very sensitive but low bandwidth)

M. L. Roukes, *Tech. Digest. Solid State Sensor and Actuator Workshop* (2000)

Promising NEMS Applications

<u>Mechanically detected magnetic resonance imaging</u>

Clinical MRI has a spatial resolution of ~1 mm since current spin detection schemes require ~10^{14} nuclei

However, a nanomagnet mounted on a NEMS device improves resolution in 2 ways:

- Only spins in close proximity to the inhomogeneous magnetic field from the nanomagnet are excited.
- The excited spins are detected with high sensitivity by the mechanical response of the NEMS device that is induced by the force exerted on the nanomagnet by the precessing spins.

M. L. Roukes, *Tech. Digest. Solid State Sensor and Actuator Workshop* (2000)

Mechanically Detected Magnetic Resonance Imaging

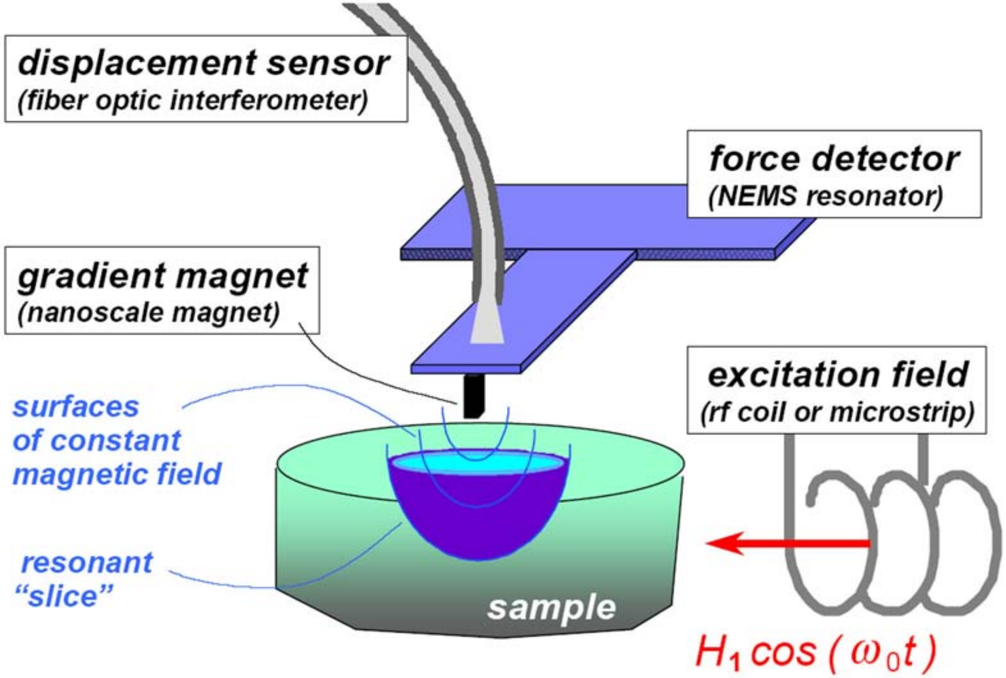

Figure 3. Schematic of the force detection approach to MRI.

M. L. Roukes, *Tech. Digest. Solid State Sensor and Actuator Workshop* (2000)